Available online at www.sciencedirect.com
ScienceDirect
Journal of the European Ceramic Society 26 (2006) 3539–3546
www.elsevier.com/locate/jeurceramsoc

# Effect of the volume ratio of zirconia and alumina on the mechanical properties of fibrous zirconia/alumina bi-phase composites prepared by co-extrusion

Hiroyuki Miyazaki *, Yu-ichi Yoshizawa, Kiyoshi Hirao

*Advanced Manufacturing Research Institute, National Institute of Advanced Industrial Science and Technology (AIST), 2266-98, Shimo-shidami, Moriyama-ku, Nagoya 463-8560, Japan*

Received 30 October 2005; received in revised form 16 December 2005; accepted 28 December 2005
Available online 20 February 2006

**Abstract**

Fibrous zirconia/alumina composites with different composition were fabricated by piston co-extrusion. After a 3rd extrusion step and sintering at 1600 °C, crack-free composites with a fibre width of ~50 μm were obtained for all compositions. The effect of the volume ratio of secondary phase on the mechanical properties was investigated. The Young's modulus of the composites decreased linearly with increasing the zirconia content. The fracture toughness of the composites was improved by introducing fine second phase filaments into the matrix. The maximum fracture toughness of 6.2 MPa $m^{1/2}$ was attained in the 3rd co-extruded 47/53 vol% zirconia/alumina composite. The improvement in toughness was attributed to both "stress-induced" transformation of zirconia and a crack deflection mechanism due to thermal expansion mismatch between the two phases. Bending strength of the composites was almost the same as that of the monolithic alumina regardless of the composition.


*Keywords:* Co-extrusion; $ZrO_2/Al_2O_3$ composite; Mechanical properties

## 1. Introduction

Continuous fibre-reinforced ceramics have promising potential for high-temperature application because of the remarkable fracture toughening through the crack bridging mechanism. However, they are very expensive, and many problems appear in the fabrication process. Different geometric configurations that incorporate crack deflecting systems, such as ceramic/ceramic lamellar composites[1] and fibrous monolithic ceramics,[2] are proposed for low-cost alternatives to conventional continuous-fiber ceramic composites. In the case of such composites, increased toughness is usually associated with the presence of a weak interface, which enables crack deflection into the interface. The weak interface, however, results in a reduction in strength. In order to maintain strength and yet obtain high toughness, lamellar composites with a strong interface were proposed, in which crack deflection was generated by thermal residual stress at the interface.[3–7] In the case of fibrous composites, there are some reports on the microstructure of the fibrous composites with a rigid interface,[8–14] but the evaluation of their mechanical properties is limited.[8–11]

In our previous reports, the feasibility of forming fine-scale fibrous microstructures was demonstrated for alumina/zirconia composites with a rigid interface, by using a repeated co-extrusion process through a reduction die.[10,11] It was revealed that fracture toughness of these composites was increased over the constituent monoliths. Lee et al. clarified the effect of number of extrusion steps on the mechanical properties of the 50/50 vol% alumina-(*m*-zirconia)/*t*-zirconia fibrous composite.[9] However, the examination of the mechanical properties of the fibrous composites has been limited to a few compositions. It seems possible to improve the mechanical properties further by optimizing the composition. The aim of this study is to clarify the effect of the volume fraction of zirconia phase on the mechanical properties of the fibrous zirconia/alumina composites.

## 2. Experimental

Commercial alumina powder (AL-160SG-4, Showa Denko K.K., Japan) and yttria-stabilized zirconia powder (TZ-3Y,

* Corresponding author. Tel.: +81 52 736 7486; fax: +81 52 736 7405.
*E-mail address:* h-miyazaki@aist.go.jp (H. Miyazaki).

0955-2219/$ – see front matter © 2006 Elsevier Ltd. All rights reserved.
doi:10.1016/j.jeurceramsoc.2005.12.019

Tosoh, Japan) were used as the starting powders. The powders were milled individually in ethanol, and the slurry was dried in a rotary evaporator. The alumina powder was tempered with distilled water, organic binders and plasticizer using a hook type mixing machine and a roller mill. Similarly, the zirconia powder was tempered with distilled water, organic binders, plasticizer and dispersant using the same apparatus. Detailed description of the mixing process for this study was reported in our previous papers.[10,11] Each of the obtained plastic bodies was extruded into a hexagonal shape by means of a screw auger machine. A total of 37 monofilaments were bundled into a hexagonal feedrod. In order to fabricate zirconia/alumina composites with different compositions, the numbers of each zirconia and alumina monofilament in the feedrod were varied in the ratio of 4/33, 12/25, 18/19, 25/12 and 33/4 (Fig. 1). The initial feedrod was extruded through a 6:1 hexagonal reduction die using a piston extruder. After the first co-extrusion, the individual pieces were bundled to create a second feedrod. The same process was repeated for the second and third co-extrusion. After the third co-extrusion, the extruded green bodies were dried at room temperature under atmospheric pressure. The dried bodies were then calcined at 600 °C for 4 h under a flow of nitrogen to remove organic substances, followed by calcining at 500 °C for 3 h in air to completely remove remaining carbon substances. After being cold isostatically pressed (CIPed) under 300 MPa, they were pressureless sintered at 1600 °C for 3 h. The final volume fractions $f_Z$ of the zirconia for each composition were 10, 31, 47, 66 and 88 vol%, respectively, which were slightly different from the values estimated from the ratio of each monofilament since the net contents of powder in the each monofilament were different. For the comparison, monolithic alumina, monolithic zirconia and powder-mixture composites (10/90, 50/50 and 90/10 vol% zirconia/alumina) were also fabricated by the same procedure.

Density measurements were conducted for both the composites and monoliths using the Archimedes technique. With dimensions of 3 mm × 4 mm × 35 mm, 9–12 specimens of each composition were machined from the sintered samples for mechanical property measurement. Four-point bending strength measurement was conducted with an inner and outer span of 10 mm and 30 mm, respectively, and a crosshead speed of 0.5 mm/min. Young's modulus was measured from the load-displacement curves which were compensated for the compliance of both the testing machine and the jig. Fracture toughness ($K_{IC}$) was determined by the single-edged-precracked-beam (SEPB) method with a span of 16 mm. Fracture strength and fracture toughness measurements, as well as Young's modulus measurements, were carried out so that tensile stress during measurements was parallel to the extruding direction. Fracture surfaces and polished surfaces of the composites were observed using scanning electron microscope and optical microscope. The grain size of sintered samples was determined by the mean linear intercept method using micrographs of polished and thermally etched surface.[15] The average grain size was calculated by multiplying the mean linear intercept by 1.78. In order to evaluate the "stress-induced" phase transformation of zirconia as well as the residual stress, X-ray diffraction analysis was conducted. It is well known that grinding induces transformation of zirconia in the surface region,[16] so that measurements of monoclinic phase before fracture were taken place on the polished surface from which the grinding-transformed layer was completely removed. The monoclinic phase after fracture was measured on the fractured surface. The volume fraction of monoclinic zirconia in the zirconia phase, $m/(m+t)$, before and after fracture was calculated according to Garvie's equation.[17] Then the volume fraction of the transformed zirconia in the composite was attained by multiplying the volume fraction of zirconia, $f_Z$. In order to estimate the residual stress in both zirconia and alumina phase caused by thermal expansion mismatch between the two phases, the full width at half maximum (FWHM) of zirconia (1 3 3) peak and alumina (1.0.10) peak was measured on the polished surface after subtraction of the contribution from $K\alpha_2$ peak. The XRD measurements were repeated for 3–4 times to attain both the average and standard deviation of FWHM.

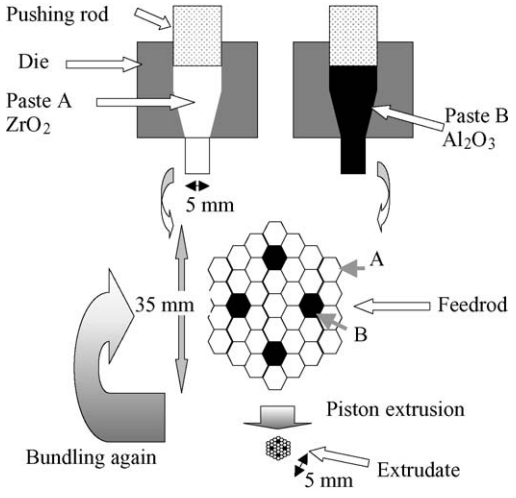


Fig. 1. Schematic illustration for fabrication of fibrous bi-phase composites by co-extrusion process.

## 3. Results and discussion

### 3.1. Microstructure and density

Fig. 2 shows optical micrographs of the composites for which $f_Z$ was 31, 47 and 66 vol%, respectively. The zirconia phase has a lighter contrast, and alumina has a darker contrast. Although the width of the phases was not uniform and interfaces were corrugated, the width of the most filaments of minor phase was reduced to ~50 μm and the number of filaments was increased significantly, close to the theoretical value expected from the number of extrusion. It is obvious that the co-extrusion process effectively reduced the width of each filament. Fine scale fibrous microstructures similar to those in Fig. 2 were also fabricated in the 10/90 vol% zirconia/alumina composite and 88/12 vol% zirconia/alumina composite by the 3rd co-extrusion process, as reported elsewhere.[10,11] Most of the filaments were not continuous after the 3rd extrusion as seen in Fig. 2. However, each phase still maintained unidirectional alignment. Cracks were not observed with an optical microscope in any of the composites.

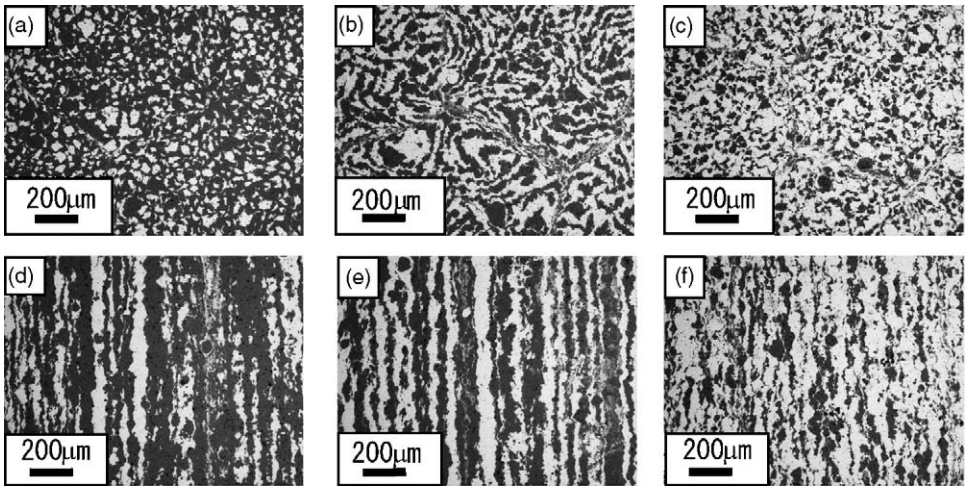


Fig. 2. Optical micrographs of both cross section (upper row) and side view (lower row) of zirconia/alumina fibrous composites sintered at 1600 °C for 3 h. The volume fraction of zirconia phase is (a) and (d): 31%; (b) and (e): 47% and (c) and (f):66%, respectively.

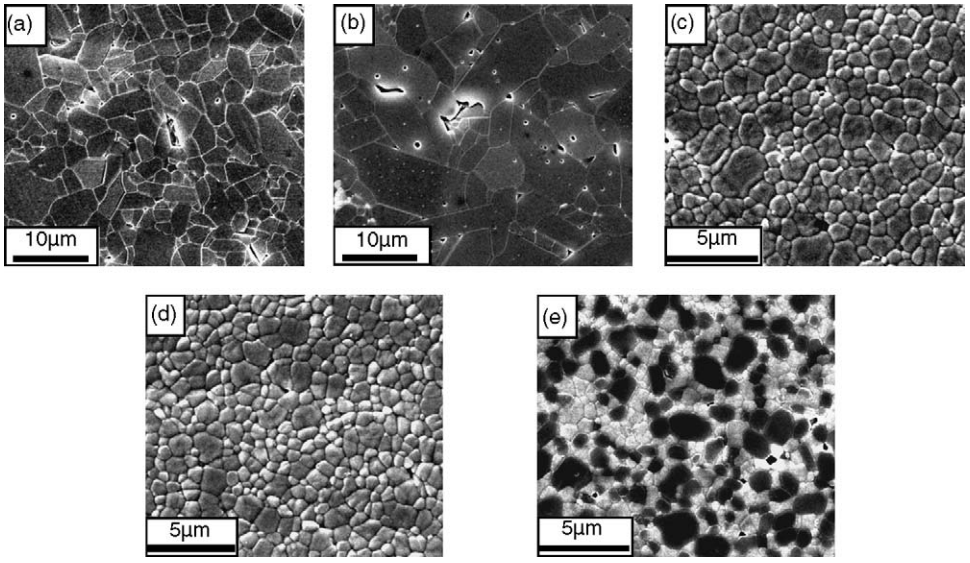


Fig. 3. SEM image of (a) alumina monolith; (b) alumina phase in 47/53 vol% zirconia/alumina fibrous composite; (c) zirconia phase in 47/53 vol% zirconia/alumina fibrous composite; (d) zirconia monolith and (e) 50/50 vol% zirconia/alumina powder-mixture composite.

Fig. 3 shows SEM micrographs of the alumina and zirconia monoliths, the fibrous composite (47 vol%-zirconia) and the powder-mixture composite (50 vol%-zirconia). In order to evaluate the microstructures of monoliths and alumina or zirconia phase in the composites quantitatively, average grain size was measured by the intercept method. Table 1 summarizes the average grain sizes of both alumina and zirconia. The average grain size of alumina in the fibrous composites was almost the same regardless of the composition and larger than that of the monolithic alumina. Xue et al. reported that $Y^{3+}$ ion enhances grain growth of alumina in the presence of glassy phase on the grain boundary which forms from silica contamination.[18] The alumina

Table 1
Average grain size of each phase and relative density of the constituent monoliths, the fibrous composites and the powder-mixture composites

| Sample | Alumina | Fibrous composites | | | | | Zirconia | Powder-mixture composites | | |
|---|---|---|---|---|---|---|---|---|---|---|
| | 0[a] | 10[a] | 31[a] | 47[a] | 66[a] | 88[a] | 100[a] | 10[a] | 50[a] | 90[a] |
| Grain size of alumina (μm) | 4.2 | 5.8 | 6.6 | 6.0 | 6.0 | 5.4 | – | 1.8 | 1.3 | 1.1 |
| Grain size of zirconia (μm) | – | 1.6 | 1.5 | 1.4 | 1.5 | 1.4 | 1.3 | 0.7 | 1.1 | 1.4 |
| Relative density (%) | 98.8 | 98.8 | 98.2 | 99.1 | 97.3 | 97.8 | 100 | 99.3 | 99.3 | 98.2 |

[a] Volume fraction of $ZrO_2$ (%).

powder used in this study contained 0.02 wt% silica. It is likely that yttrium in the zirconia phase may have diffused into the alumina phase and affected the grain growth of alumina. By contrast, the size of alumina grain in the powder-mixture composites decreased significantly with increasing the zirconia content. The inhibition of grain growth in matrix phase by addition of secondary phase particles is well known as "pinning effect".[19–21] The grain growth of alumina in the powder-mixture composites was inhibited by the pining effect of the zirconia particles. The grain size of zirconia in the fibrous composites was almost the same as that of the monolithic zirconia. The size of zirconia grain in the powder-mixture composites decreased with increasing the alumina content because of the pinning effect by alumina particles.

Both the monolithic alumina and monolithic zirconia were sintered to almost full density (Table 1), whereas the relative density of the composites was slightly lower than that of the monolithic. The insufficient densification in these fibrous composites may arise from mismatch in both the total amount of sintering shrinkage and the shrinkage rate between the two phases.

### 3.2. Young's modulus

Fig. 4 shows the dependence of the Young's modulus on the $f_Z$ for both the fibrous composites and the powder-mixture composites. The solid line in the Fig. 4 shows the calculated value using the well-known Voigt rule-of-mixture:

$$E = E_z f_z + E_a(1 - f_z) \quad (1)$$

where $E_z$ and $E_a$ are the Young's modulus of zirconia and alumina and $f_Z$ is the volume fraction of the zirconia phase. The Young's modulus, $E_z$ and $E_a$, used for the calculation was measured with the alumina and zirconia monoliths, respectively. From Fig. 4, it is clear that the Young's modulus of both the fibrous composites and powder-mixture composites followed the Voigt rule-of-mixture. The measured value was slightly lower than the predicted value, which is attributable to the lower relative densities of the composites.

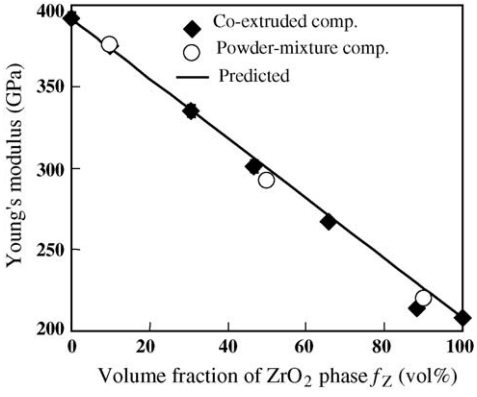


Fig. 4. Dependence of the Young's modulus of both co-extruded composites and powder-mixture composites on the volume fraction of zirconia phase $f_Z$.

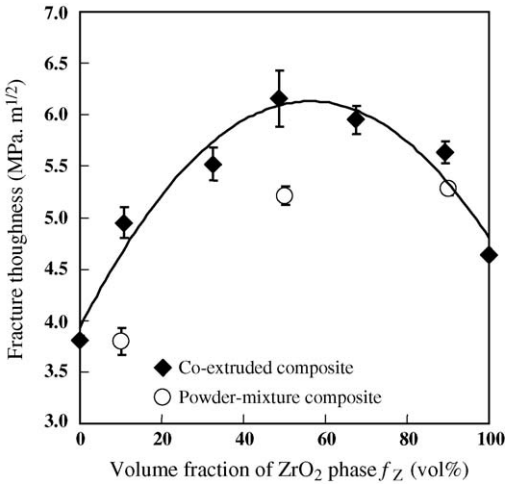


Fig. 5. Dependence of the fracture toughness of the composites on the volume fraction of zirconia phase $f_Z$.

### 3.3. Fracture toughness

#### 3.3.1. Effect of "stress-induced" transformation of zirconia on the fracture toughness

Fig. 5 shows the fracture toughness of both the composites and the constituent monolithic ceramics. The fracture toughness of the powder-mixture composites was almost the same as that of the monolithic alumina when the $f_Z$ was 10 vol%, and increased with $f_Z$, then became saturated at the higher $f_Z$. To correlate toughness with the tetragonal-to-monoclinic transformation, the volume fraction of the transformed zirconia phase in the composites due to fracture was measured. The result is shown in Fig. 6 along with the data for the fibrous composites. The volume fraction of transformed zirconia in the powder-mixture composites was very small when $f_Z$ was 10 vol%, and increased with $f_Z$. It is obvious that the improvement in fracture toughness of the powder-mixture composites was originated mainly from the "stress-induced" transformation of zirconia phase.

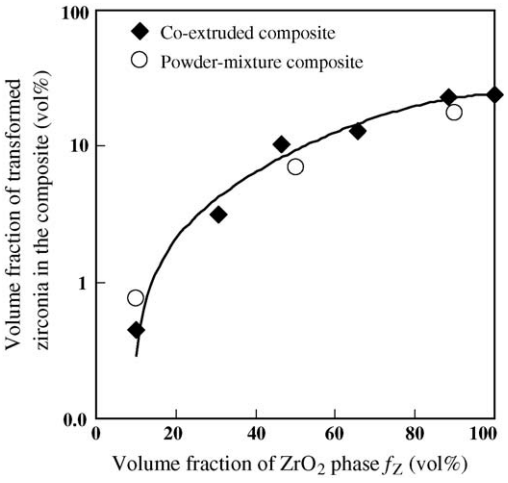


Fig. 6. Volume fraction of zirconia transformed from tetragonal to monoclinic in both co-extruded composites and powder-mixture composites as a function of volume fraction of zirconia phase $f_Z$.

By contrast, the fracture toughness of the fibrous composites was increased even by introducing a small amount of fine zirconia filaments into alumina matrix (Fig. 5), and was further increased with $f_Z$ and reached a maximum (6.2 MPa $m^{1/2}$) where $f_Z$ was 47 vol%. Then the fracture toughness decreased slightly with $f_Z$ but still maintained higher value than that of the monolithic zirconia. The volume fractions of transformed zirconia in the fibrous composites are shown in Fig. 6 (solid square). The volume fraction of transformed zirconia in the fibrous composites increased with $f_Z$, which was almost the same rising curve behavior as that of the powder-mixture composites. It is reasonable to suppose that contribution from the "stress-induced" transformation to the toughness of the fibrous composites was almost the same level as that of the powder-mixture composites. Consequently, the higher fracture toughness of the fibrous composites over that of powder-mixture composites is attributed to another toughening mechanism.

### 3.3.2. *Effect of crack deflection mechanism on the fracture toughness*

Fig. 7 shows crack propagation of an indenter-induced crack on both the 47/53 vol% zirconia/alumina fibrous composite and the 50/50 vol% zirconia/alumina powder-mixture composite. Crack deflection at the zirconia/alumina interface was observed in the fibrous composite, whereas crack deflection was not observed by an optical microscope in the powder-mixture composite. The same result was also obtained at the 10/90 vol% zirconia/alumina composite.[10] It is clear that the residual stress produced by mismatch of thermal expansion between alumina and zirconia affected the crack propagation more effectively in the case of fibrous microstructure further increasing the fracture toughness. Although the composites have the fibrous microstructure, pullout of the fine fibrous second phase was not observed (Fig. 8). The lack of pullout of the fibrous phase is due to a tough bonding at the interface between the two phases.

The decrease in toughness of the fibrous composites with $f_Z$ over 47 vol% (Fig. 5), despite the increased volume fraction of transformed zirconia (Fig. 6), implies that the contribution from the "crack-deflection" mechanism caused by residual stress decreased. The contribution of the crack-deflection mechanism to the increment in fracture toughness of the fibrous composite can be estimated by the product of the frequency of interaction between the crack and the second phase, which causes crack deflection, and the effect of a crack deflection at an interface between the fiber and the matrix. The frequency of interaction between the crack and the second phase is represented by the volume fraction of the second phase providing the width of the second phase filaments is constant. Adachi et al. reported that the degree of the crack deflection in the alumina/zirconia biphase lamer composite increased with increasing the difference of residual stress between the two phases.[7] It is reasonable to assume that the effect of a crack deflection on the toughness is almost proportional to the variation in the residual stress across the interface. Then the dependence of the increment in toughness due to the crack-deflecting mechanism on $f_Z$ can be analyzed by the product of the volume fraction of the secondary phase and the difference of the residual stress between the fiber and the matrix. The residual thermal stress in the fiber-reinforced composites was analyzed by Budiansky et al., by using the composite cylinder model.[22] The average of residual stress of matrix is given by the following equation.

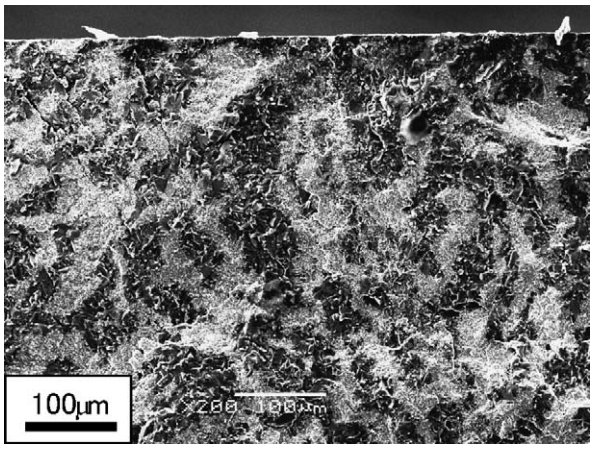


Fig. 8. SEM image of fracture surface of the 47/53 vol% zirconia/alumina co-extruded composite. No trace of the pullout of fibers was observed.

$$\frac{\sigma_m}{E_m} = \frac{\lambda_2}{\lambda_1}\left[\frac{E_f}{E}\right]\left[\frac{c_f}{1-\nu_m}\right]\Omega \tag{2}$$

where $\sigma$ is axial stress, $E$ the Young's modulus, $c$ the volume fraction, $\nu$ Poisson's ratio and subscripts m and f refer to matrix and fiber, respectively. $\lambda_1$ and $\lambda_2$ are functions of $c_m$, $E_m/E_f$, $\nu_m$ and $\nu_f$ shown explicitly in appendix. $\Omega$ is the thermal strain

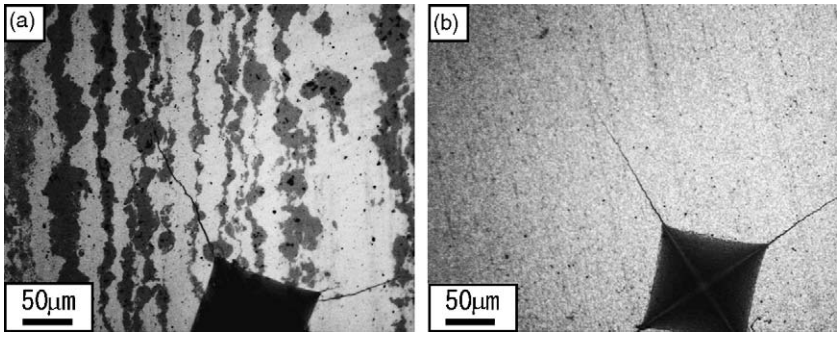


Fig. 7. Propagation of crack generated by indentation in (a) 47/53 vol% zirconia/alumina co-extruded composite and (b) 50/50 vol% zirconia/alumina powder-mixture composite. The indentation load was 196 N for (a) and 98 N for (b).

Table 2
Material property data for alumina and zirconia

| | Alumina | Zirconia |
|---|---|---|
| Young's modulus, $E$ (GPa) | 390 | 210 |
| Poisson's ratio, $\nu$ | 0.25 | 0.3 |
| Coeff. of thermal expansion, $\alpha$ ($^\circ C^{-1}$) | $8.3 \times 10^{-6}$ | $10 \times 10^{-6}$ |

given by

$$\Omega = (\alpha_f - \alpha_m)\Delta T \quad (3)$$

where $\alpha_f$ and $\alpha_m$ are the coefficients of thermal expansion of fiber and matrix, $\Delta T$ is the temperature difference over which the residual thermal stress develops in the composites.

The average of residual thermal stress in fiber is given by

$$\frac{\sigma_f}{E_f} = -\frac{\lambda_2}{\lambda_1}\left[\frac{E_m}{E}\right]\left[\frac{c_m}{1-\nu_m}\right]\Omega \quad (4)$$

The thermal residual stresses in both the alumina and zirconia phases were calculated with the above equations by substituting the physical properties data for the two materials (see Table 2) and assuming $\Delta T = 1000\,^\circ C$.[3,7] When $f_Z$ is 47 vol%, both the alumina and zirconia phases were neither matrix nor fiber since they had nearly same volume content and were not covered by each other (Fig. 2 (b)). Then the average residual stresses in both the alumina and zirconia phases were calculated for both the fiber and matrix cases. The result is shown in Fig. 9. It was found that the calculated residual stress in the alumina phase was always compressive and proportional to the volume fraction of zirconia. It was also shown that the residual stress in the zirconia phase was always tensile and proportional to the volume fraction of alumina. The discontinuity in both the residual stress curves at $f_Z = 47$ vol% is due to the switching of the zirconia fiber to the zirconia matrix. It is revealed that the difference in residual stress between the two phases is almost constant regardless of the composition.

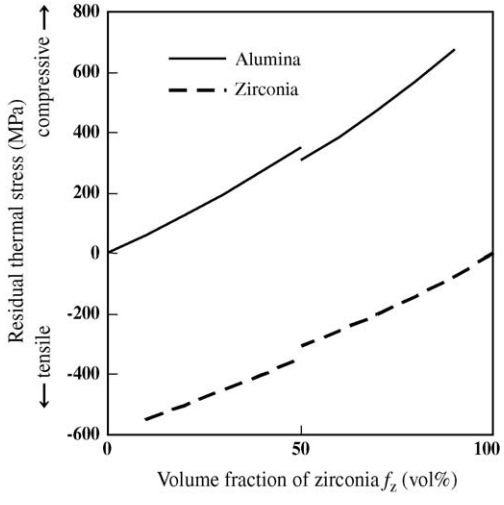


Fig. 9. Average of residual thermal stress in both alumina and zirconia phases as a function of volume fraction of zirconia, $f_Z$, calculated with the Eqs. (2)–(4) and the physical data in Table 2. Compressive stress is positive and tensile stress is negative in the figure.

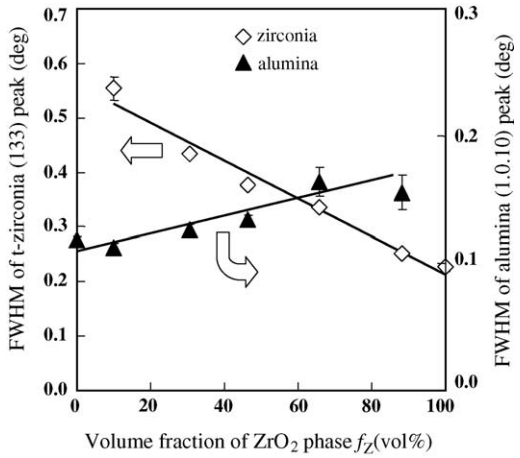


Fig. 10. Full width at half maximum (FWHM) of XRD peaks of tetragonal zirconia (1 3 3) and alumina (1.0.10) reflections in the fibrous composites as a function of volume fraction of zirconia phase $f_Z$.

In order to confirm the above calculation of the residual stresses in both the alumina and zirconia phases experimentally, FWHM of the XRD peak of both alumina (1.0.10) reflection and zirconia (1 3 3) reflection was measured. The FWHM of both the alumina and zirconia is shown in Fig. 10 as a function of $f_Z$. The FWHM of the alumina peak increased with $f_Z$, suggesting that the residual stress in alumina increased, while the FWHM of the zirconia peak decreased with increasing $f_Z$, suggesting that the residual stress in zirconia decreased, which is consistent with the above calculation (Fig. 9). Then the above estimation of the difference in residual stress between the two phases is also reasonable. The effect of crack deflection per a fiber/matrix interface on the toughness is supposed to be nearly constant in every composition. The volume fraction of the secondary zirconia phase is maximum at $f_Z = 47$ vol% when $f_Z \leqq 47$ vol%. Similarly, when $f_Z \geqq 47$ vol%, the volume fraction of the secondary alumina phase is maximum at $f_Z = 47$ vol%. Then the product of the volume fraction of the secondary phase and the effect of crack deflection at a fiber/matrix interface has maximum at $f_Z = 47$ vol%, which means the increment in fracture toughness due to the crack deflection mechanism should reach maximum at $f_Z = 47$ vol%. Thus, the reason of the fracture toughness having maximum value at $f_Z = 47$ vol% was explained by the estimation of the residual stresses in the two phases.

### 3.4. Bending strength

Table 3 shows the bending strength and the Weibull modulus of both the fibrous and powder-mixture composites, as well as the constituent monoliths. The strength of the fibrous composites was almost the same as that of the monolithic alumina, whereas the Weibull modulus of the fibrous composites was improved. The increase in Weibull modulus of these composites is attributable to the increment in the fracture toughness,

Table 3
4-point bending strength and Weibull modulus of the fibrous composites, the powder-mixture composites and constituent monoliths

| Sample | Alumina | Fibrous composites | | | | | Zirconia | Powder-mixture composites | | |
|---|---|---|---|---|---|---|---|---|---|---|
| | 0[a] | 10[a] | 31[a] | 47[a] | 66[a] | 88[a] | 100[a] | 10[a] | 50[a] | 90[a] |
| Average strength (MPa) | 496 | 434 | 478 | 545 | 567 | 586 | 859 | 637 | 891 | 878 |
| S.D. (MPa) | 40 | 13 | 31 | 28 | 33 | 58 | 134 | 123 | 97 | 105 |
| Weibull modulus | 11 | 30 | 15 | 19 | 18 | 10 | 6 | 5 | 9 | 8 |
| No. | 9 | 9 | 9 | 9 | 9 | 10 | 11 | 12 | 11 | 10 |

S.D.: standard deviation; No.: number of specimen.
[a] Volume fraction of $ZrO_2$ (%).

since the strength becomes less sensitive to the distribution of flaw size when its fracture toughness increases. The fact that there was no significant increase in strength of the composites over that of the monolithic alumina, despite the improved fracture toughness, suggests that the flaw size in the composites was larger than that in the monolithic alumina. It is reasonable to suppose that the mismatch in sintering behavior between the two phases not only inhibited full densification of the composites but also introduced the fracture origin, which lowered the strength. Although the fracture toughness of the powder-mixture composites was lower than those of the fibrous composites, the strength of the powder-mixture composites was higher than that of the fibrous composites, which indicates that the flaw size in the powder-mixture composites was smaller than that of the fibrous composites. The decrease in flaw size in the powder-mixture composites is contributed to the fact that the grain size in the powder-mixture composites was much finer than that in the fibrous composites.

## 4. Conclusion

Fibrous zirconia/alumina composites with different compositions were fabricated by piston co-extrusion. A fine-scale and aligned microstructure with no thermal cracking was obtained for all the compositions following three extrusion steps. The Young's modulus of the composites followed the well-known Voigt rule-of-mixture. All these composites attained higher toughness than that of the constituent monolithic ceramics with no degradation in the bending strength. The fracture toughness was optimized at the composition of 47/53 vol% zirconia/alumina and the maximum fracture toughness of 6.2 MPa $m^{1/2}$ was attained. The effect of the aligned fibrous microstructure on the toughness improvement was through a crack deflection mechanism produced by thermal residual stress at the interface, as well as by "stress-induced" transformation of zirconia. The variation in the fracture toughness among these composites was explained by the variation in the contributions from each mechanism. The Weibull modulus of the fibrous composites increased owing to the increment in fracture toughness, while the strength remained almost the same as that of monolithic alumina, indicating that favorable influence of the increased fracture toughness was offsetted by the increment in the flaw size.

## Appendix A

$\lambda_1$ and $\lambda_2$ are defined as follows.

$$\lambda_1 = \frac{1-(1-E/E_f)(1-\nu_f)/2 + c_m(\nu_m-\nu_f)/2 - (E/E_f)\left[\nu_f+(\nu_m-\nu_f)c_f E_f/E\right]^2}{(1-\nu_m)\Delta}, \quad (A.1)$$

$$\lambda_2 = \frac{\left[1-(1-E/E_f)/2\right](1+\nu_f)+(1+c_f)(\nu_m-\nu_f)/2}{\Delta}, \quad (A.2)$$

where

$$\Delta = 1+\nu_f+\frac{(\nu_m-\nu_f)c_f E_f}{E} \quad (A.3)$$

and

$$E = c_f E_f + c_m E_m \quad (A.4)$$

## References


1. Clegg, W. J., Kendall, K., McN. Alford, N., Button, T. W. and Birchall, J. D., A simple way to make tough ceramics. *Nature*, 1990, **347**, 455–457.
2. Kovar, D., King, B. H., Trice, R. W. and Halloran, J. W., Fibrous monolithic ceramics. *J. Am. Ceram. Soc.*, 1997, **80**, 2471–2487.
3. Prakash, O., Sarkar, P. and Nicholson, P. S., Crack deflection in ceramic/ceramic laminates with strong interfaces. *J. Am. Ceram. Soc.*, 1995, **78**, 1125–1127.
4. Menon, M. and Chen, I. W., Bimaterial composites vie colloidal rolling techniques: III, mechanical properties. *J. Am. Ceram. Soc.*, 1999, **82**, 3430–3440.
5. Rao, M. P., Sánchez-Herencia, A. J., Beltz, G. E., McMeeking, R. M. and Lange, F. F., Laminar ceramics that exhibit a threshold strength. *Science*, 1999, **286**, 102–105.
6. Dakskobler, A., Kosmač, T. and Chen, I. W., Paraffin-based process for producing layered composites with cellular microstructures. *J. Am. Ceram. Soc.*, 2002, **85**, 1013–1015.
7. Adachi, T., Sekino, T., Kusunose, T., Nakayama, T., Hikasa, A., Choa, Y. H. and Niihara, K., Crack propagation behavior of nano-sized SiC dispersed multilayered $Al_2O_3$/3Y-TZP hybrid composites. *J. Ceram. Soc. Jpn*, 2003, **111**, 4–7.
8. Poulon-Quintin, A., Berger, M. H., Bunsell, A. R., Kaya, C., Butler, E. G., Wootton, A. *et al.*, Processing and structures of bi-phase oxide ceramic filaments. *J. Eur. Ceram. Soc.*, 2004, **24**, 101–110.
9. Lee, B. T., Kim, K. H. and Han, J. K., Microstructures and material properties of fibrous $Al_2O_3$-(*m*-$ZrO_2$)/*t*-$ZrO_2$ composites fabricated by a fibrous monolithic process. *J. Mater. Res.*, 2004, **19**, 3234–3241.

10. Miyazaki, H., Yoshizawa, Y. and Hirao, K., Preparation and mechanical properties of 10 vol% zirconia/alumina composite with fine-scale fibrous microstructure by co-extrusion process. *Mater. Lett.*, 2004, **58**, 1410–1414.
11. Miyazaki, H., Yoshizawa, Y. and Hirao, K., Fabrication of fibrous bimaterial composite by a co-extrusion process. *J. Ceram. Soc. Jpn. Suppl.*, 2004, **112**, S130–S133.
12. Kaya, C., Butler, E. G. and Lewis, M. H., Co-extrusion of $Al_2O_3/ZrO_2$ bi-phase high temperature ceramics with fine scale aligned microstructure. *J. Eur. Ceram. Soc.*, 2003, **23**, 935–942.
13. Kaya, C., Butler, E. G. and Lewis, M. H., Microfabrication of $Al_2O_3/ZrO_2$ bi-phase ceramics with continuous fibrillar microstructure by co-extrusion. *J. Mater. Sci. Lett.*, 2003, **22**, 357–361.
14. Kim, T. S., Kim, K. H., Goto, T. and Lee, B. T., Microstructure control of $Al_2O_3/ZrO_2$ composite by fibrous monolithic process. *Mater. Trans.*, 2004, **45**, 431–434.
15. Mendelson, M. I., Average grain size in polycrystalline ceramics. *J. Am. Ceram. Soc.*, 1969, **52**, 443–446.
16. Garvie, R. C., Hannink, R. H. and Pascoe, R. T., Ceramic steel? *Nature*, 1975, **258**, 703–704.
17. Garvie, R. C. and Nicholson, P. S., Phase analysis in zirconia systems. *J. Am. Ceram. Soc.*, 1972, **55**, 303–305.
18. Xue, L. A., Meyer, K. and Chen, I. W., Control of grain-boundary pinning in $Al_2O_3/ZrO_2$ composite with $Ce^{3+}/Ce^{4+}$ doping. *J. Am. Ceram. Soc.*, 1992, **75**, 822–829.
19. Lange, F. F. and Hirlinger, M. M., Grain growth in two-phase ceramics: $Al_2O_3$ inclusion in $ZrO_2$. *J. Am. Ceram. Soc.*, 1987, **70**, 827–830.
20. Lange, F. F. and Hirlinger, M. M., Hindrance of grain growth in $Al_2O_3$ by $ZrO_2$ inclusions. *J. Am. Ceram. Soc.*, 1984, **67**, 164–168.
21. Okada, K., Yoshizawa, Y. and Sakuma, T., Grain-size distribution in $Al_2O_3$—$ZrO_2$ generated by high-temperature annealing. *J. Am. Ceram. Soc.*, 1991, **74**, 2820–2823.
22. Budiansky, B., Hutchinson, J. W. and Evans, A. G., Matrix fracture in fiber-reinforced ceramics. *J. Mech. Phys. Solids.*, 1986, **34**, 167–189.